A time-variant analysis of the 1/f^(2) phase noise in CMOS parallel LC-Tank quadrature oscillators

Andreani, Pietro

Published in:
I E E E Transactions on Circuits and Systems Part 1: Regular Papers

Link to article, DOI:
10.1109/TCSI.2006.879011

Publication date:
2006

Document Version
Publisher's PDF, also known as Version of record

A Time-Variant Analysis of the $1/f^2$ Phase Noise in CMOS Parallel *LC*-Tank Quadrature Oscillators

Pietro Andreani, *Member, IEEE*

***Abstract*—This paper presents a study of $1/f^2$ phase noise in quadrature oscillators built by connecting two differential *LC*-tank oscillators in a parallel fashion. The analysis clearly demonstrates the necessity of adopting a time-variant theory of phase noise, where a more simplistic, time-invariant approach fails to explain numerical simulation results even at the qualitative level. Two topologies of 5-GHz parallel quadrature oscillators are considered, and compact but nevertheless highly general, closed-form formulas are derived for the phase noise caused by the losses in the *LC*-tanks and by the noisy currents in the MOS transistors. A large number of spectreRF simulations, covering a wide range of working conditions for the oscillators, is used to validate the theoretical analysis.**

***Index Terms*—CMOS, *LC*-tank, oscillators, phase noise, quadrature.**

I. Introduction

WHILE powerful simulators such as spectreRF have enabled designers of integrated oscillators to estimate very quickly the phase noise performances of any oscillator topology, allowing design optimization over a very large set of parameters, the numerical nature of such results makes it difficult to understand how the different noise sources in the circuit contribute to the overall phase noise. It is therefore sometimes important to arrive at a deeper understanding of the mechanisms by which noise is converted into phase noise, gaining those design insights that only the traditional approach to circuit analysis is able to provide. In the last few years, many important results have been obtained in this sense, among which we can mention the study of the tail noise [1]–[3] and transistor noise [2]–[4] in differential *LC*-tank oscillators, the impact of varactor nonlinearities [5], [6], and closed-form phase-noise formulas in CMOS Colpitts oscillators [4], [7].

Quadrature *LC*-tank oscillators have also attracted a great deal of attention (see e.g., [8]–[13]), since quadrature phases from the local oscillator are needed in all modern radio transceivers. An important result for this class of oscillators has been obtained by Romanò *et al.*, who have produced the expression of the phase noise generated by the tank resistances for a popular *LC*-tank parallel quadrature oscillator (PQO) design [14].

The goal of this paper is to study the conversion of noise into phase noise for both tank noise and transistor noise in the two most popular implementations of *LC*-tank PQOs. Closed-form formulas will be derived, and, perhaps equally important from a theoretical point of view, the nontrivial nature of the analysis and the importance of adopting a time-variant approach in the study of oscillator phase noise will become apparent. The treatment will be couched in terms of Hajimiri's theory of phase noise [15] because of its elegant simplicity and intuitiveness, although we will have to transcend it, in order to derive closed-form symbolic expressions.

The paper is organized as follows. Section II presents the two PQOs treated in this work, and shows how the simpler arguments used in the phase noise analysis of the differential *LC*-tank oscillator are inadequate, if extended to the PQOs. Section III introduces the time-variant approach employed in all subsequent calculations of phase noise, together with the fundamental formulas quantifying the amount of white noise that is converted into phase noise. Sections IV and V contain the analysis of the two PQOs, respectively, deriving closed-form expression for the phase noise caused by the most important white noise sources. Section VI summarizes the main results obtained in this work, while the Appendix presents a formal derivation of the formulas stated in Section III.

II. Parallel *LC*-Tank Oscillators

Two PQOs will be treated in this paper, portrayed in Figs. 1 and 2, respectively, where the parallel tank resistance R accounts for all losses in each tank in the proximity of the resonance frequency. The PQO in Fig. 1 is composed of two differential *LC*-tank oscillators, coupled to each other through two additional differential pairs. Quadrature oscillation is achieved by the combination of direct-coupling and cross-coupling between the two differential oscillators (otherwise they would oscillate in phase, acting as a single differential oscillator). The PQO in Fig. 2 is identical to that in Fig. 1, the only difference being that the sources of each switching pair (defined as usual as the transistor pair belonging to the original differential oscillator) are connected to the sources of the respective coupling pair.[1] For this reason, in the following, we will refer to the first PQO as the disconnected-sources PQO (dsPQO), and to the second as the connected-sources PQO (csPQO).

A. Attempt at a Time-Invariant Phase Noise Analysis, and Its Failure

An analysis of the phase noise generated by both the switching and coupling transistors (to be referred to hereafter

Manuscript received December 19, 2005; revised March 31, 2006. This paper was recommended by Associate Editor J. R. Chen.

The author is with the Center for Physical Electronics, Ørsted·DTU, Technical University of Denmark, DK-2800 Kgs. Lyngby, Denmark (e-mail: pa@oersted.dtu.dk).

Digital Object Identifier 10.1109/TCSI.2006.879011

[1]However, this seemingly trivial circuit difference results in a very significant difference in the phase accuracy of the two architectures, when the unavoidable component mismatches are considered. This important subject will be treated at length in a different paper [16].

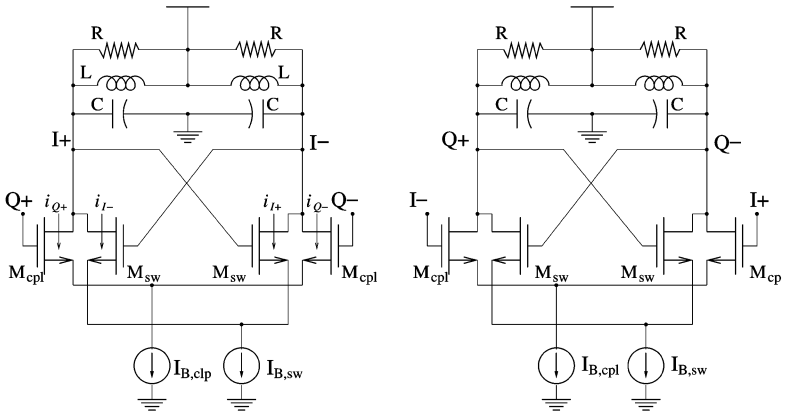

Fig. 1. Simplified schematic view of the dsPQO.

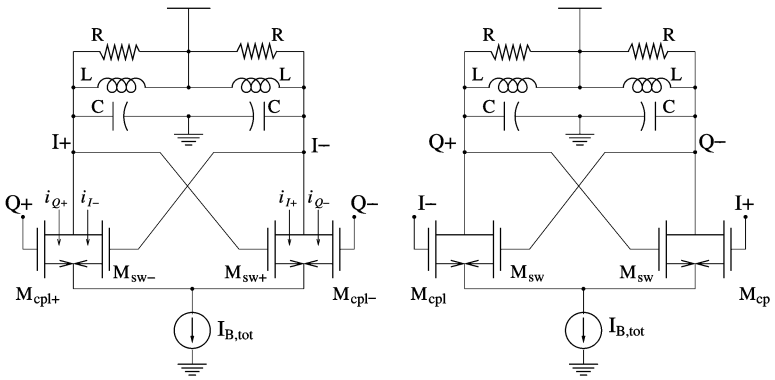

Fig. 2. Simplified schematic view of the csPQO.

as $M_{\rm sw}$ and $M_{\rm cpl}$) might try to utilize what is already known about the differential *LC*-tank oscillator. After all, each half of the dsPQO is made of two differential pairs that do not interact with each other, and can therefore be treated separately. In the following, we will also assume that the voltages at the transistor gates are sinusoidal, which is (almost) true as long as the quality factor Q of the tanks is at least moderately high.

We start by defining the parameter k as

$$k = \frac{I_{B,\rm cpl}}{I_{B,\rm sw}} \tag{1}$$

where $I_{B,\rm sw}$ $(I_{B,\rm cpl})$ is the tail current for each switching (coupling) pair, see Fig. 1. The width of $M_{\rm cpl}$ and $M_{\rm sw}$ in the dsPQO will be scaled accordingly, even though it will be shown that this has (ideally) no effect on the oscillator behavior. Fig. 3 shows the voltage and current waveforms for a dsPQO built around four identical *RLC* tanks having a self-resonance frequency of 5 GHz, an inductance value of 1 nH, a Q of 15, and $I_{B,\rm cpl} = I_{B,\rm sw} = 2$ mA (i.e., $k = 1$). The transistor model employed is quite ideal, which explains why the current waveforms look so square-wave-like; this simplification, however, is necessary, if we do not want to be overwhelmed by a host of second-order effects. Fortunately, the results we are going to obtain can be applied to the general case, qualitatively if not quantitatively.

Turning again to Fig. 3, it is obvious as well as expected that the current delivered by the switching pair is in phase with the voltage at the gates of the switching transistors, while the current delivered by the coupling pair is in quadrature with the same voltage. Therefore, one might be tempted to apply the same argument usually invoked [2] when analyzing the differential *LC*-tank oscillator: the switching transistors contribute to phase noise only when the pair is commutating, and this happens exactly when the phase of the tank voltage waveforms is most sensitive to disturbances. Thus, all noise from the switching pair is converted into phase noise, which leads to the (correct) conclusion [2], [3] that the phase noise caused by the tank resistances and the phase noise caused by the switching transistors, respectively, are in a ratio of $1 : \gamma$, where γ is the channel noise factor of the MOS transistor.

The coupling transistors, on the other hand, are injecting noise into the tank only when the phase of the tank voltages is least sensitive to disturbances (or so goes the argument). The coupling transistors noise does cause amplitude noise on the oscillation, but this is rejected by the internal amplitude-stabilizing mechanism of the oscillator. From this analysis, one would expect that the phase noise in the dsPQO is mainly caused by the tank resistances and the switching transistors (in a proportion $1 : \gamma$), while the impact of the coupling transistors is almost negligible. In fact, spectreRF simulations show that, for $k = 1$, coupling and switching transistors contribute roughly the same amount of phase noise, and tank resistors and switching transistors, respectively, contribute in a proportion much lower than $1 : \gamma$, and very close to $1 : \gamma/2$ (where $\gamma = 2/3$ in the long-channel limit).

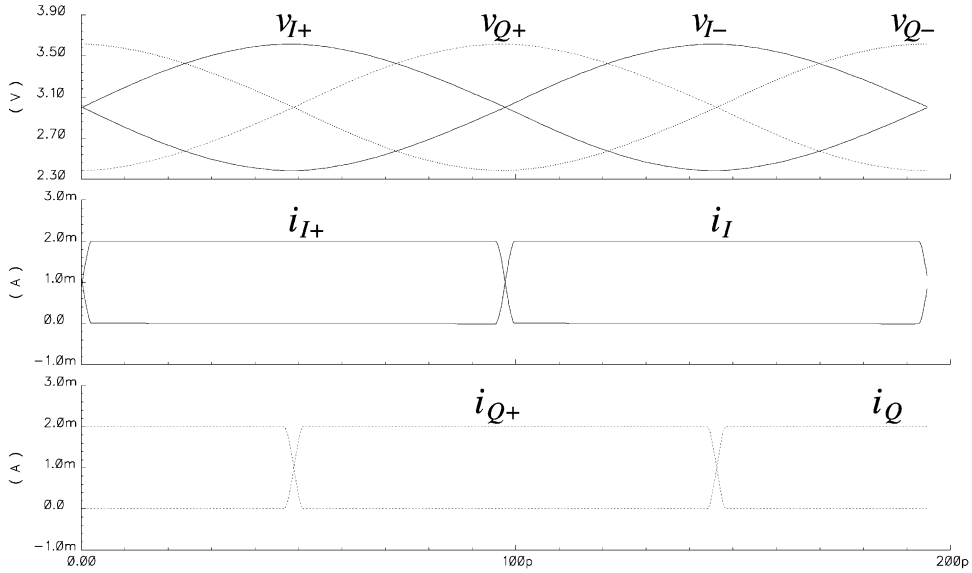

Fig. 3. Voltage and current waveforms for the I-half of the dsPQO in Fig. 1.

TABLE I
SIMULATED NOISE CONTRIBUTIONS (IN $10^{-15} \cdot V^2_{rms}$/Hz) AT 1-MHz OFFSET FREQUENCY FROM THE CARRIER, FOR EACH TANK RESISTANCE R, SWITCH TRANSISTOR M_{sw}, AND COUPLING TRANSISTOR M_{cpl} (CALLED $N_{\mathcal{L},i_R}$, $N_{\mathcal{L},i_{I+}}$, AND $N_{\mathcal{L},i_{Q-}}$, RESPECTIVELY), IN THE 5-GHz dsPQO OF FIG. 1

k	1/4	1/3	1/2	1	2	3	4
$N_{\mathcal{L},i_R}$	7.1	7.5	8.4	13.3	32.1	62.0	103
$N_{\mathcal{L},i_{I+}}$	4.4	4.5	4.5	4.6	5.0	5.5	6.5
$N_{\mathcal{L},i_{Q-}}$	0.05	0.14	0.48	4.0	30.7	98.7	225
$N_{\mathcal{L},i_R}$	15.4%	15.4%	15.7%	15.2%	11.8%	9.3%	7.7%
$N_{\mathcal{L},i_{I+}}$	9.5%	9.3%	8.4%	5.2%	1.8%	0.9%	0.5%
$N_{\mathcal{L},i_{Q-}}$	0.1%	0.3%	0.9%	4.6%	11.4%	14.8%	16.8%

In order to try to get a more complete picture of the dsPQO behavior, a number of spectreRF simulations were run for different values of k (keeping a constant $I_{B,sw}$ of 2 mA), with the results reported in Table I. SpectreRF expresses any noise contribution to phase noise as a phase-noise-generating noise $N_{\mathcal{L}}$ defined by the relation

$$\mathcal{L} = 10 \log \left(\frac{N_{\mathcal{L}}}{A^2/2} \right) \tag{2}$$

where $\mathcal{L}$ is the phase noise, and $A^2/2$ is the power of the oscillation voltage, assumed sinusoidal with peak value A, at the node where the phase noise is measured (the phase noise itself is independent of the node where it is measured, while $N_{\mathcal{L}}$ does depend on it [13]).

It is clear that, for the lowest values of k, the relative noise contributions from R, M_{sw}, and M_{cpl} (called $N_{\mathcal{L},i_R}$, $N_{\mathcal{L},i_{I+}}$, and $N_{\mathcal{L},i_{Q-}}$, respectively), are quite close to the expected ones: the ratio of $N_{\mathcal{L},i_R}$ to $N_{\mathcal{L},i_{I+}}$ is roughly $1:\gamma$, and $N_{\mathcal{L},i_{Q-}}$ is negligible. Moreover, it is easy to realize that the ratio of $N_{\mathcal{L},i_{Q-}}$ to $N_{\mathcal{L},i_{I+}}$ is much smaller than the ratio of the respective transistor channel noise. This is because most of the noise from M_{cpl} does not translate into phase noise, as previously stated.

For larger values of k, however, the situation becomes very different, and simulation results do not conform to expectations any longer: the relative impact of $N_{\mathcal{L},i_{I+}}$ does not remain constant, but decreases to negligibility; $N_{\mathcal{L},i_{Q-}}$, on the other hand, grows to eventually dominate, and its growth is this time larger than what would be accounted for by the increasing channel noise only. Finally, the absolute values of the different $N_{\mathcal{L}}$ contributions increase with k, except $N_{\mathcal{L},i_{I+}}$, which remains almost constant. It is therefore very obvious that our simple analysis fails badly in the general case, and our goal is now to find one able to explain all data in Table I.

As a matter of fact, as previously mentioned, Romanò *et al.* have already treated the case of the tank noise as a function of k [14], finding the formula (in the notation of this paper)

$$\mathcal{L}_{R,k} = (1 + k^2)\mathcal{L}_{R,k=0} \tag{3}$$

which yields the correct amount of phase noise generated by R for all values of k. Our approach will recover the same result, together with the expressions for the phase noise contributed by the transistors.

III. TIME-VARIANT PHASE-NOISE ANALYSIS

It is quite straightforward to find out whether the seemingly innocent assumption made in the phase noise analysis of the previous section, i.e., that the switching transistors noise is totally converted into phase noise, as is indeed the case in differential oscillators, is correct or not. This can be done by injecting a small disturbance into an oscillator node (e.g., a current impulse charging a tank capacitor), and then measuring the phase deviation of the perturbed waveform from a reference waveform. By sweeping the instant when the disturbance is injected across a whole oscillation period, it is possible to get quite an accurate picture of when the phase of the waveform is most sensitive to noise. In fact, many readers will have recognized the outlined procedure as the cornerstone in Hajimiri's and Lee's impulse

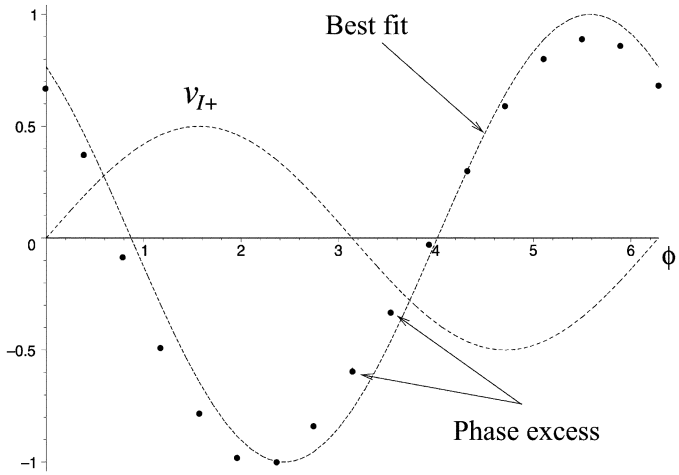

Fig. 4. Normalized phase excess for the voltage $v_{I+} = A\sin(\phi)$ at node $I+$ of the dsPQO, when a delta-like current impulse is injected into the same node. The best sinusoidal fit for the 16 simulated values is $\cos(\phi + 46°)$.

sensitivity function (ISF, with symbol Γ) linear-time-variant approach to the study of phase noise [15], [17], which for the first time gave a simple and nevertheless very accurate way of calculating the phase noise in a general oscillator, by means of a number of standard transient simulations. For a short period of time the ISF was the only practical way to study the phase noise in a theoretically correct way, before the advent of modern simulators rendered the task trivial.

It is well known [15], [13] that in a differential *LC*-tank oscillator the ISF is sinusoidal and in quadrature with the voltage at the node where it is calculated, and that this form for the ISF explains the various phase noise contributions in such oscillators. Turning to the dsPQO, Fig. 4 shows the normalized phase excess, caused by a small current impulse injected into node $I+$, together with the relative node voltage, again for $k = 1$. While the phase excess is very well approximated by a sinusoid, there is in this case a substantial departure from quadrature; in fact, the best sinusoidal fit for the data has a 46° phase shift from quadrature. A few more numerical simulations lead us to the following conjecture: a good approximation of the phase shift Ψ from ideal quadrature undergone by the ISF is

$$\Psi = \arctan(k). \tag{4}$$

In the Appendix we will show that this conjecture is indeed correct, the approximated expressions for the ISFs being

$$\Gamma_{I+}(\phi) = -\Gamma_{I-}(\phi) = \frac{1}{N\cos(\Psi)}\cos(\phi + \Psi) \tag{5}$$

$$\Gamma_{Q+}(\phi) = -\Gamma_{Q-}(\phi) = \frac{1}{N\cos(\Psi)}\sin(\phi + \Psi) \tag{6}$$

where $N(=4)$ is the number of *LC*-tanks in the quadrature oscillator,[2] and where we have assumed that the node voltages have the form

$$v_{I+}(\phi) = -v_{I-}(\phi) = A\sin(\phi) \tag{7}$$

$$v_{Q+}(\phi) = -v_{Q-}(\phi) = -A\cos(\phi). \tag{8}$$

[2]For small values of Ψ, (5) and (6) reduce to $\Gamma_{I+}(\phi) \approx \cos(\phi)/N$ and $\Gamma_{Q+}(\phi) \approx \sin(\phi)/N$, which have already been derived in [13]. Equations (5) and (6) can therefore be considered as the extension to the general case of the partial results contained in [13].

The angle $0 \le \phi \le 2\pi$ is used instead of $\omega_1 t$ for simplicity, ω_1 being the angular frequency of oscillation. In the following, we will show that (5)–(6), simple as they are, are all we need to reconcile simulation results with theoretical predictions.

IV. Phase Noise Analysis of the dsPQO

Referring to a general oscillator, it has been shown [15], [17] that the phase noise $\mathcal{L}$ at the offset frequency $\Delta\omega$, measured between one oscillator node and ground, is given by

$$\mathcal{L}(\Delta\omega) = 10\log\left(\sum_j \frac{\Gamma_{j,\mathrm{rms}}^2}{q_{\max}^2}\cdot\frac{\overline{i_j^2}/\Delta f}{2\Delta\omega^2}\right) \tag{9}$$

where $\Gamma_{j,\mathrm{rms}}$ is the root-mean-square value of the ISF Γ_j associated to the stationary white noise current i_j, and $q_{\max}$ is the maximum amount of dynamic charge loaded onto the capacitance between the oscillator node and ground; all noise currents are assumed uncorrelated to one another. When a cyclo-stationary noise source is considered, the same (9), valid for stationary noise sources, can still be applied, provided that the ISF is replaced by an effective ISF Γ_{eff}, defined as [15]

$$\Gamma_{\mathrm{eff}}(\phi) = \Gamma(\phi)\cdot\alpha(\phi) \tag{10}$$

where $\alpha(\phi)$ includes the dependence of the noise source power on ϕ.

The phase noise treatment in the quadrature oscillators is very similar to the one followed in [4] for the analysis of the differential *LC*-tank oscillator, albeit more complicated. In order to make the present paper somewhat self-contained, we will repeat here some of the details of the approach.

Due to the symmetry of the quadrature oscillator, we focus on the I-part of it, all results being transferable to the Q-part via a 90° phase shift. In fact, it will be enough to calculate the phase-noise contribution of just one-half of the I-part, again because of symmetry. Therefore, we will concentrate on what happens at node $I-$ (Fig. 1); the total phase noise can thereafter be calculated as [13]

$$\mathcal{L} = 10\log\left(N\cdot\frac{N_{\mathcal{L},i_R} + N_{\mathcal{L},i_{I+}} + N_{\mathcal{L},i_{Q-}}}{A^2/2}\right) \tag{11}$$

where all quantities are referred to node $I-$ (to repeat, $\mathcal{L}$ is independent of this choice [13]).

A. Tank Losses

We start by considering the simple case of the noise generated by the tank losses, whose stationary white noise current is given by the well-known expression

$$\overline{i_R^2} = 4k_B T\frac{1}{R}\Delta f \tag{12}$$

where k_B is Boltzmann's constant, T is the absolute temperature, R is the equivalent parallel tank resistance accounting for all tank losses, and Γ_{R_t} is the ISF of such a noise source. However, Γ_{R_t} is, by definition, the same as Γ_{I-} in (5); therefore, the square rms value of Γ_{i_R} is

$$\Gamma_{i_R,\mathrm{rms}}^2 = \int_{-\pi}^{\pi}\Gamma_{I-}^2(\phi)d\phi = \frac{1}{2N^2\cos^2(\Psi)}. \tag{13}$$

Combining (2), (9), and (13), and making use of the relation $q_{\max} = CA$, we obtain

$$\begin{aligned} N_{\mathcal{L},i_R} &= \frac{\Gamma_{i_R,\mathrm{rms}}^2 \overline{i_R^2}/\Delta f}{2q_{\max}^2 \Delta\omega^2} \cdot \frac{A^2}{2} \\ &= \frac{4k_BT(1/R)}{2N^2\cos^2(\Psi)} \frac{1}{2C^2A^2\Delta\omega^2} \cdot \frac{A^2}{2} \\ &= \frac{k_BT}{2RC^2N^2\cos^2(\Psi)\Delta\omega^2}. \end{aligned} \tag{14}$$

However, the trigonometric relation

$$\frac{1}{\cos^2(\Psi)} = \frac{1}{\cos^2(\arctan(k))} = 1 + k^2 \tag{15}$$

shows that (13) is in perfect accordance with (3), since the amplitude of the oscillation is

$$A \approx \frac{2}{\pi} I_{B,\mathrm{sw}} R \tag{16}$$

independently of k (see also the Appendix 1).

B. Switching Transistors

Let us now turn to the more difficult treatment of the transistor noise. As previously mentioned, switching pair and coupling pair are independent of each other, so that they can be studied separately. Calling i_{I+} and i_{I-} the currents in the switching pair (see Fig. 1), and neglecting all parasitic components at the common source, we obtain

$$i_{I-}(\phi) + i_{I+}(\phi) = I_{B,\mathrm{sw}}. \tag{17}$$

The above equation, together with (7)–(8), results, after some simple algebraic manipulations [4], in

$$i_{I+}(\phi) = \frac{\beta_{\mathrm{sw}}}{2} A^2 (\sin(\phi) + \sqrt{2\sin^2(\Phi_{\mathrm{sw}}) - \sin^2(\phi)})^2 \tag{18}$$

$$i_{I-}(\phi) = \frac{\beta_{\mathrm{sw}}}{2} A^2 (-\sin(\phi) + \sqrt{2\sin^2(\Phi_{\mathrm{sw}}) - \sin^2(\phi)})^2 \tag{19}$$

where $\beta_{\mathrm{sw}} = \mu_e C_{\mathrm{ox}} W_{\mathrm{sw}}/L_{\mathrm{sw}}$ (μ_e being the electron mobility, C_{ox} the gate oxide capacitance per unit area, and W_{sw} and L_{sw} the transistor width and length, respectively), and where

$$\Phi_{\mathrm{sw}} = \arcsin\sqrt{\frac{I_{B,\mathrm{sw}}}{2\beta_{\mathrm{sw}}A^2}}. \tag{20}$$

Φ_{sw} divides the operation mode of the differential pair into two regions: for $-\Phi_{\mathrm{sw}} < \phi < \Phi_{\mathrm{sw}}$ or $\pi - \Phi_{\mathrm{sw}} < \phi < \pi + \Phi_{\mathrm{sw}}$, both transistors are working in saturation; otherwise, one of them is turned off. From (18)–(19), the transconductances of the switching transistors are given by

$$g_{m_{I+}}(\phi) = \beta_{\mathrm{sw}} A (\sin(\phi) + \sqrt{2\sin^2(\Phi_{\mathrm{sw}}) - \sin^2(\phi)}) \tag{21}$$

$$g_{m_{I-}}(\phi) = \beta_{\mathrm{sw}} A (-\sin(\phi) + \sqrt{2\sin^2(\Phi_{\mathrm{sw}}) - \sin^2(\phi)}). \tag{22}$$

We make now use of the result demonstrated in [4], which states that the ISF $\Gamma_{i_{I+}}$ of the noise current $i_{n,I+}$ displayed by i_{I+} is

$$\Gamma_{i_{I+}}(\phi) = \Gamma_{I-}(\phi) \frac{2g_{m_{I-}}(\phi)}{g_{m_{I+}}(\phi) + g_{m_{I-}}(\phi)} \tag{23}$$

where a commonly used expression for the power of $i_{n,I+}$ is

$$\begin{aligned} \overline{i_{n,I+}^2} &= 4k_BT\gamma g_{m_{I+}} \Delta f = 4k_BT\gamma\beta_{\mathrm{sw}} A \\ &\quad \times (\sin(\phi) + \sqrt{2\sin^2(\Phi_{\mathrm{sw}}) - \sin^2(\phi)})\Delta f \\ &\equiv \overline{i_{n,I+}'^2} \alpha^2(\phi) \end{aligned} \tag{24}$$

with

$$\overline{i_{n,I+}'^2} = 4k_BT\gamma\beta_{\mathrm{sw}} A \Delta f \tag{25}$$

and

$$\alpha(\phi) = \sqrt{\sin(\phi) + \sqrt{2\sin^2(\Phi_{\mathrm{sw}}) - \sin^2(\phi)}} \tag{26}$$

and where the simplifying assumption is made that $\overline{i_{n,I+}^2}$ is proportional to $g_{m_{I+}}$ through γ.

From (10), (24), and (26), the effective ISF for $i_{n,I+}$ becomes

$$\begin{aligned} \Gamma_{i_{I+},\mathrm{eff}}(\phi) &= \frac{-\cos(\phi+\Psi)}{N\cos(\Psi)} \frac{2g_{m_{I-}}(\phi)}{g_{m_{I+}}(\phi) + g_{m_{I-}}(\phi)} \\ &\quad \times \sqrt{\sin(\phi) + \sqrt{2\sin^2(\Phi_{\mathrm{sw}}) - \sin^2(\phi)}}. \end{aligned} \tag{27}$$

After a few simplifications, $\Gamma_{i_{I+},\mathrm{eff},\mathrm{rms}}^2$ can be written as

$$\begin{aligned} \Gamma_{i_{I+},\mathrm{eff},\mathrm{rms}}^2(\Psi) &= \frac{1}{2\pi} \int_{-\Phi_{\mathrm{sw}}}^{2\pi-\Phi_{\mathrm{sw}}} \Gamma_{i_{I+},\mathrm{eff}}(\phi)\, d\phi \\ &= \frac{1}{\pi N^2 \cos^2(\Psi)} g_I(\Psi, \Phi_{\mathrm{sw}}) \end{aligned} \tag{28}$$

where

$$\begin{aligned} g_I(\Psi, \Phi_{\mathrm{sw}}) &= \int_{-\Phi_{\mathrm{sw}}}^{\Phi_{\mathrm{sw}}} \cos^2(\phi+\Psi) f(\phi, \Phi_{\mathrm{sw}})\, d\phi \\ &\quad + \int_{\pi-\Phi_{\mathrm{sw}}}^{\pi+\Phi_{\mathrm{sw}}} \cos^2(\phi+\Psi) f(\phi, \Phi_{\mathrm{sw}})\, d\phi \end{aligned} \tag{29}$$

and

$$\begin{aligned} f(\phi, \Phi_{\mathrm{sw}}) &= \frac{-\sin(\phi) + \sqrt{2\sin^2(\Phi_{\mathrm{sw}}) - \sin^2(\phi)}}{2\sin^2(\Phi_{\mathrm{sw}}) - \sin^2(\phi)} \\ &\quad \times (\sin^2(\Phi_{\mathrm{sw}}) - \sin^2(\phi)). \end{aligned} \tag{30}$$

It has been shown [4] that, for $\Psi = 0$, the following relation (with the notation adopted in this work) is an almost exact solution of (29)

$$g_I(0, \Phi_{\mathrm{sw}}) = 2\sin^2(\Phi_{\mathrm{sw}}) = \frac{I_{B,\mathrm{sw}}}{\beta_{\mathrm{sw}} A^2}. \tag{31}$$

Further, we can express the factor $\cos(\phi+\Psi)$ under the integral sign in (29) as

$$\cos(\phi+\Psi) = \cos(\phi)\cos(\Psi) - \sin(\phi)\sin(\Psi) \tag{32}$$

TABLE II
SIMULATED/CALCULATED NOISE CONTRIBUTIONS (IN $10^{-15} \cdot V^2_{rms}$/Hz) AT 1-MHz OFFSET FREQUENCY FROM THE CARRIER, FOR EACH R, M_{sw}, AND M_{cpl} IN THE 5-GHz dsPQO OF FIG. 1

k	1/4	1/3	1/2	1	2	3	4
$N_{\mathcal{L},i_R}$	7.1/7.1	7.5/7.5	8.4/8.4	13.3/13.5	32.1/33.8	62.0/67.6	103/115
$N_{\mathcal{L},i_{I+}}$	4.4/4.5	4.5/4.5	4.5/4.5	4.6/4.5	5.0/4.5	5.5/4.5	6.5/4.6
$N_{\mathcal{L},i_{Q-}}$	0.05/0.07	0.14/0.16	0.48/0.56	4.0/4.5	30.7/36.0	98.7/121	225/288

and notice that, for small values of $-\Phi_{sw} \le \phi \le \Phi_{sw}$, the term in $\sin(\phi)$ is negligible compared to the term in $\cos(\phi)$; therefore, (29) can be simplified as

$$g_I(\Psi, \Phi_{sw}) \approx \cos^2(\Psi) g_I(0, \Phi_{sw}) = \cos^2(\Psi) \frac{I_{B,sw}}{\beta_{sw} A^2}. \tag{33}$$

From (2), (9), (16), (28), and (33), the final equation for $N_{\mathcal{L},i_{I+}}$ is

$$\begin{aligned} N_{\mathcal{L},i_{I+}} &= \frac{\Gamma^2_{i_{I+},eff,rms}(\Psi)\overline{i'^2_{n,I+}}/\Delta f}{2q^2_{max}\Delta\omega^2} \cdot \frac{A^2}{2} \\ &= \frac{I_{B,sw}}{\pi N^2 \beta_{sw} A^2} \frac{4k_B T\gamma\beta_{sw} A}{2C^2A^2\Delta\omega^2} \cdot \frac{A^2}{2} \\ &= \frac{k_B T\gamma}{2RC^2N^2\Delta\omega^2}. \end{aligned} \tag{34}$$

The above equation proves that $N_{\mathcal{L},i_{I+}}$ is (ideally) independent of k, as was strongly suggested by Table I.

C. Coupling Transistors

Looking again at Fig. 1, it is clear that we can repeat the whole treatment of the previous section for the coupling pair as well, provided that all equations for transistor currents, transconductances, and noise are time shifted by $T/4$ (i.e., phase shifted by $\pi/2$), and that $I_{B,sw}$ is substituted with $I_{B,cpl}$. The only equation that should not be phase shifted is $\Gamma_{I-}(\phi)$ in (23), as $\Gamma_{I-}(\phi)$ is the same for all noise sources flowing into node $I-$.

We are, however, not so much interested in the transistor equations *per se*, but rather in the final value of $\Gamma^2_{i_{Q-},eff,rms}$, to be obtained with the same procedure that lead to (28). Therefore, we can exploit the fact that all the phase shifted equations figure under the integration sign, by performing a $\pi/2$ phase shift of the integration variable. In this way, we can reuse most of the results obtained in the previous section, once in (27)–(30) we substitute $\Gamma_{I-}(\phi)$ with $\Gamma_{I-}(\phi+\pi/2)$, β_{sw} with β_{cpl}, $I_{B,sw}$ with $I_{B,cpl}$, and Φ_{sw} with Φ_{cpl}, where

$$\Phi_{cpl} = \arcsin\sqrt{\frac{I_{B,cpl}}{2\beta_{cpl}A^2}} = \arcsin\sqrt{\frac{kI_{B,sw}}{2\beta_{cpl}A^2}}. \tag{35}$$

In particular, reusing (29) we obtain quickly $g_Q(\Psi, \Phi_{cpl})$ as

$$\begin{aligned} g_Q(\Psi, \Phi_{cpl}) = &\int_{-\Phi_{cpl}}^{\Phi_{cpl}} \cos^2\left(\phi + \Psi + \frac{\pi}{2}\right) f(\phi, \Phi_{cpl})\, d\phi \\ &+ \int_{\pi-\Phi_{cpl}}^{\pi+\Phi_{cpl}} \cos^2\left(\phi + \Psi + \frac{\pi}{2}\right) f(\phi, \Phi_{cpl})\, d\phi. \end{aligned} \tag{36}$$

Again, $\cos(\phi) \gg \sin(\phi)$ for small values of $-\Phi_{cpl} \le \phi \le \Phi_{cpl}$, and (36) results in

$$\begin{aligned} g_Q(\Psi, \Phi_{cpl}) &\approx 2\cos^2\left(\Psi + \frac{\pi}{2}\right) g_I(0, \Phi_{cpl}) \\ &= 2\sin^2(\Psi)\, g_I(0, \Phi_{cpl}) \\ &= \sin^2(\Psi) \frac{kI_{B,sw}}{\beta_{cpl}A^2}. \end{aligned} \tag{37}$$

From (2), (9), (16), (28), and (37), the final equation for $N_{\mathcal{L},i_{Q-}}$ is

$$\begin{aligned} N_{\mathcal{L},i_{Q-}} &= \frac{\Gamma^2_{i_{Q-},eff,rms}(\Psi)\overline{i'^2_{n,Q-}}/\Delta f}{2q^2_{max}\Delta\omega^2} \cdot \frac{A^2}{2} \\ &= \frac{kI_{B,sw}\sin^2(\Psi)}{\pi N^2\cos^2(\Psi)\beta_{cpl}A^2} \frac{4k_B T\gamma\beta_{cpl}A}{2C^2A^2\Delta\omega^2} \cdot \frac{A^2}{2} \end{aligned} \tag{38}$$

which is easily simplified to

$$N_{\mathcal{L},i_{Q-}} = k^3 \frac{k_B T\gamma}{2RC^2N^2\Delta\omega^2} \tag{39}$$

given the relation

$$\frac{\sin^2(\Psi)}{\cos^2(\Psi)} = \tan^2(\Psi) = [\tan(\arctan(k))]^2 = k^2. \tag{40}$$

It is noteworthy that $N_{\mathcal{L},i_{Q-}}$ does not depend on β_{cpl}, as $N_{\mathcal{L},i_{I+}}$ did not depend on β_{sw}; however, $N_{\mathcal{L},i_{Q-}}$ is a very strong function of k, while we have seen that $N_{\mathcal{L},i_{I+}}$ is independent of it. This was again expected from Table I.

From (14), (34), and (38), we find that the ratios of the three phase-noise-generating noise powers are very simple functions of k

$$N_{\mathcal{L},i_R} : N_{\mathcal{L},i_{I+}} : N_{\mathcal{L},i_{Q-}} = (1+k^2) : \gamma : k^3\gamma. \tag{41}$$

Table II shows the values of $N_{\mathcal{L},i_R}$, $N_{\mathcal{L},i_{I+}}$, and $N_{\mathcal{L},i_{Q-}}$, for several values of k, calculated by means of the previously derived equations, together with the simulated values. The agreement between calculations and simulations is excellent for $N_{\mathcal{L},i_R}$ and $N_{\mathcal{L},i_{I+}}$, while the (small) discrepancies in $N_{\mathcal{L},i_{Q-}}$ are most likely due to the presence of higher-order harmonics in the full expression of $\Gamma_{i_{Q-}}$.

V. PHASE NOISE ANALYSIS OF THE CSPQO

A. Current Waveforms in the csPQO

Although the csPQO looks superficially very similar to the dsPQO, the current waveforms in the two oscillators are in reality very different. As shown in Figs. 3 and 5, if switch and coupling transistors have the same dimensions, each transistor in the csPQO conducts the whole tail current (which in this case

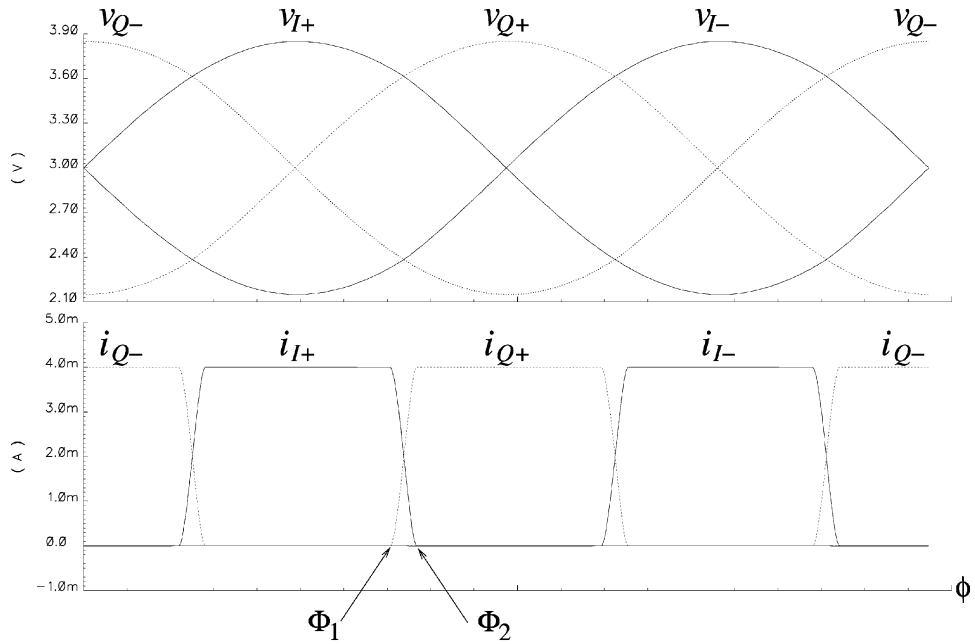

Fig. 5. Voltage and current waveforms for the I-half of the csPQO in Fig. 2.

is obviously common for all four transistors) for one fourth of the period. Incidentally, this way of operation also means that the conversion of the dc bias current into the first harmonic of the tank current in phase with the tank voltage (called hereafter $I_{1\mathrm{st},I+}$, while we call $I_{1\mathrm{st},Q+}$ the first harmonic of the tank current in quadrature with the tank voltage) is more efficient in the csPQO than in the dsPQO. In fact, from Fig. 5 we obtain

$$I_{1\mathrm{st},I+} = \frac{1}{\pi}\int_0^{2\pi} i_{I+}(\phi)\sin(\phi)d\phi \approx \frac{1}{\pi}\int_{\pi/4}^{3\pi/4} I_{B,\mathrm{tot}}\sin(\phi)d\phi = \frac{\sqrt{2}}{\pi}I_{B,\mathrm{tot}}. \quad (42)$$

Considering that, for a fair comparison, we must have $I_{B,\mathrm{tot}} = I_{B,\mathrm{sw}} + kI_{B,\mathrm{cpl}} = 2I_{B,\mathrm{sw}}$ ($k = 1$ because of symmetry), it is clear that $I_{1\mathrm{st},I+}$ is a factor $\sqrt{2}$ larger in the csPQO than in the dsPQO.

A very significant difference between csPQO and dsPQO is that changing the ratio between $I_{1\mathrm{st},I+}$ and $I_{1\mathrm{st},Q+}$ is much less straightforward in the csPQO, since here the two currents are not neatly separated in two noninteracting differential pairs. Defining the effective coupling factor k_{eff} as

$$k_{\mathrm{eff}} = \frac{I_{1\mathrm{st},Q+}}{I_{1\mathrm{st},I+}} \quad (43)$$

we can, to some extent, vary k_{eff} by varying k_n, defined as the ratio of the width W_{cpl} of M_{cpl} to the width W_{sw} of M_{sw} (assuming that all transistor lengths are identical):

$$k_n = \frac{W_{\mathrm{cpl}}}{W_{\mathrm{sw}}}. \quad (44)$$

Jumping over the somewhat tedious but elementary derivations of the formulas, the amplitude of $I_{1\mathrm{st},I+}$ is found to be (assuming square-wave-like waveforms)

$$I_{1\mathrm{st},I+} = \frac{\sqrt{2}}{\pi}I_{B,\mathrm{tot}}(\sqrt{1-\alpha^2}-\alpha) \quad (45)$$

while the amplitude of $I_{1\mathrm{st},Q+}$ is

$$I_{1\mathrm{st},Q+} = \frac{\sqrt{2}}{\pi}I_{B,\mathrm{tot}}(\sqrt{1-\alpha^2}+\alpha) \quad (46)$$

where α is defined as

$$\alpha = \frac{I_{B,\mathrm{tot}}}{\sqrt{2}A}\left(\frac{1}{\beta_{\mathrm{sw}}} - \frac{1}{\beta_{\mathrm{cpl}}}\right). \quad (47)$$

To calculate the phase noise generated by the transistors, we must again find the expressions for the transistor currents during transitions. As an example, during the transition from Φ_1 to Φ_2, indicated in Fig. 5, the equations for $i_{I+}(\phi)$ and $i_{Q+}(\phi)$ are (omitting again intermediate calculations)

$$i_{I+}(\phi) = \frac{\beta_{\mathrm{sw}}}{2}A^2(\sin(\phi)+f_s(\phi))^2 \quad (48)$$

and

$$i_{Q+}(\phi) = \frac{\beta_{\mathrm{cpl}}}{2}A^2(-\cos(\phi)+f_s(\phi))^2 \quad (49)$$

with

$$f_s(\phi) = \frac{k_n\cos(\phi)-\sin(\phi)}{1+k_n} + \frac{\sqrt{-k_n(\cos(\phi)+\sin(\phi))^2+2(1+k_n)b_{\mathrm{sw}}^2}}{1+k_n} \quad (50)$$

and

$$b_{\mathrm{sw}} = \frac{1}{A}\sqrt{\frac{I_{B,\mathrm{tot}}}{\beta_{\mathrm{sw}}}}, \quad b_{\mathrm{cpl}} = \frac{1}{A}\sqrt{\frac{I_{B,\mathrm{tot}}}{\beta_{\mathrm{cpl}}}}. \quad (51)$$

TABLE III
SIMULATED/CALCULATED NOISE CONTRIBUTIONS (IN $10^{-15} \cdot V^2_{rms}$/Hz) AT 1-MHz OFFSET FREQUENCY FROM THE CARRIER, FOR EACH R, M_{sw}, AND M_{cpl} IN THE 5-GHz csPQO OF FIG. 2

k_n	1/4	1/3	1/2	1	2	3	4
$N_{\mathcal{L},i_R}$	10.5/11.5	11.2/11.9	12.4/12.6	14.4/13.6	16.3/14.4	17.3/14.9	17.8/15.2
$N_{\mathcal{L},i_{I+}}$	4.3/5.2	5.1/5.7	6.3/6.7	8.5/8.6	11.2/10.9	13.2/12.2	14.5/13.2
$N_{\mathcal{L},i_{Q-}}$	8.0/8.9	8.3/8.8	8.7/8.8	9.3/8.6	9.3/8.1	9.1/7.6	8.7/7.3

Equations (48)–(50) are valid for $\Phi_1 \leq \phi \leq \Phi_2$, with

$$\Phi_1 = \frac{3}{4}\pi - \arcsin(b_{\rm sw}), \quad \Phi_2 = \frac{3}{4}\pi + \arcsin(b_{\rm cpl}). \quad (52)$$

B. Phase Noise in the csPQO

Looking again at Figs. 2 and 5, we notice that each transistor generates noise only during *one* current transition, and not during both, as was the case in the dsPQO. To understand why, we consider e.g., $M_{\rm sw+}$, and notice that when the tail current switches from $M_{\rm cpl-}$ to $M_{\rm sw+}$, no noise is injected into the tank, since these two transistors are in parallel to each other, and the net noise they inject into the tank is zero, because of the cascode effect from the common source node. When the current switches from $M_{\rm sw+}$ to $M_{\rm cpl+}$, on the other hand, noise is injected into the two tanks, in the same fashion as in the dsPQO case. Thus, this transition does create phase noise.

Phase noise calculations for the csPQO are of course very similar to those for the dsPQO. We assume again that the ISFs are as in (5)–(6), with Ψ given by

$$\Psi = \arctan(k_{\rm eff}). \quad (53)$$

Considering how $N_{\mathcal{L},i_R}$ was derived in (12)–(14), it is clear that $N_{\mathcal{L},i_R}$ is the same in both csPQO and dsPQO (for identical values of Ψ, of course). However, this is not to say that the phase noise generated by $\overline{i_R^2}$ is the same as well, since we have seen that the oscillation amplitude is in general different in the two oscillator. To repeat, for the same current consumption and for $k = k_n = 1$, the oscillation amplitude is $\sqrt{2}$ higher in the csPQO, resulting, via (2), in a 3-dB lower phase noise for this noise source.

The phase noise contributions from the transistors are calculated repeating exactly the same procedure followed for the dsPQO. As an example, the effective ISF for $\overline{i^2_{n,I+}}$ during the transition from Φ_1 to Φ_2 (Fig. 5) is

$$\Gamma_{i_{I+},\rm eff}(\phi) = \frac{-\cos(\phi+\Psi)}{N\cos(\Psi)} \frac{2g_{m_{Q+}}(\phi)}{g_{m_{Q+}}(\phi)+g_{m_{I+}}(\phi)} \times \sqrt{(\sin(\phi)+f_s(\phi))} \quad (54)$$

where $g_{m_{Q+}}$ and $g_{m_{I+}}$ are immediately derived from (48)–(49). It is worth noticing that, although this transition is the only time when $\overline{i^2_{n,I+}}$ produces phase noise, it does so when the absolute value of $\Gamma_{I-}(\phi)$ is at a maximum, as is clear from (5) with $\Psi = \arctan(1) = \pi/4$.

From (54), it is straightforward to calculate $\Gamma^2_{i_{I+},\rm eff,rms}$, and subsequently the phase noise caused by $\overline{i^2_{n,I+}}$. The above procedure is then repeated for $\overline{i^2_{n,Q+}}$, and for all other transitions. Table III shows a comparison between calculations (this time all integrals have been evaluated numerically) and simulations of phase noise contributions in a csPQO, for various values of the nominal coupling factor k_n. The values of the tank components are the same as in the dsPQO case; further, $\beta_{\rm sw} \approx 1$ A/V^2, and $\beta_{\rm cpl} = k_n \beta_{\rm sw}$. As is clear from the table, theory and simulations match again very well. It is interesting to notice that, for $k_n = 1$, the three noise sources are very nearly in the proportions

$$N_{\mathcal{L},i_R} : N_{\mathcal{L},i_{I+}} : N_{\mathcal{L},i_{Q-}} \approx 1 : \gamma : \gamma. \quad (55)$$

Indeed, with some patience and Maple's help, it is possible to show that, for $k_n = 1$ and small values of $b_{\rm sw} = b_{\rm cpl}$, the equalities

$$N_{\mathcal{L},i_{I+}} = N_{\mathcal{L},i_{Q-}} = \gamma N_{\mathcal{L},i_R} = \frac{k_B T \gamma}{RC^2 N^2 \Delta\omega^2} \quad (56)$$

are very good approximations of the exact values for $N_{\mathcal{L},i_R}$, $N_{\mathcal{L},i_{I+}}$, and $N_{\mathcal{L},i_{Q-}}$.

VI. CONCLUSION

The importance of adopting a time-variant theory in the study of phase noise has been made evident through the analysis of two topologies of quadrature *LC*-tank oscillators. While a straightforward, time-invariant approach failed even at the qualitative level, the time-variant treatment employed in this work resulted in a number of compact and accurate closed-form formulas for the phase noise generated by the most important white noise sources in the oscillator cores. These formulas are able to account very well for the extensive numerical simulation results used to benchmark the study.

APPENDIX

Equations (5)–(6) will be formally derived in this Appendix. To do this, we resort to a more powerful (although far less intuitive) theory than Hajimiri's, namely Kärtner's[3] [19]. Although applied to the specific case of the dsPQO, it is clear that the approach is valid in the general case, enabling in principle the symbolic analysis of phase noise in any kind of autonomous circuits (we may mention here the several PQO architectures contained in the reference list), provided that sensible simplifications are possible. For this reason, we believe it is of interest to show a worked-out example of the application of the theory. In the following, we will use Kärtner's original treatment and notation wherever possible, and notably in (57)–(61).

An oscillator is a dynamic system, described by the set of nonlinear differential equations

$$\dot{\vec{x}} = \vec{F}(\vec{x}, t, \vec{\xi}) \quad (57)$$

[3]Our phase noise analysis in [13] made use of yet another paper by Kärtner, namely [18].

where $\vec{x}$ is the vector of the state variables (i.e., voltages across capacitors and currents through inductors), and $\vec{\xi}$ is the vector of the noise sources. Let us define the components of a matrix DF as

$$DF(\vec{x}^0)_{ij} = \left.\frac{\partial F_i(\vec{x})}{\partial x_j}\right|_{\vec{x}=\vec{x}^0} \tag{58}$$

and let $\vec{y}$ be the steady-state solution of the adjoint system

$$(\dot{\vec{y}})^T = -(\vec{y})^T \cdot DF. \tag{59}$$

It is possible to show that

$$(\dot{\vec{x}})^T \cdot \vec{y} = 1 \tag{60}$$

and, most importantly, that

$$\dot{\theta}(t) = (\vec{y})^T \vec{\xi} \tag{61}$$

where $\theta(t)$ is the excess phase caused by the noise vector [19].

It is clear that the vector $\vec{y}$ in Kärtner's theory plays a role analogous to the ISFs in Hajimiri's theory. Without entering into the rather lengthy details of the derivation, it is possible to show that, for a (quasi)-sinusoidal oscillation of amplitude A and angular frequency ω, the following identity is valid:

$$\Gamma_i = A\omega y_i \tag{62}$$

where Γ_i is the ISF relative to circuital node i, and y_i is the component of $\vec{y}$ relative to the same node.

A. Phase Noise Analysis of the Single-Ended dsPQO

In the following, we are going to derive (62) for the dsPQO, and show that it yields (5)–(6). We treat for simplicity the case when only two quadrature signals are generated (i.e., a single-ended architecture, see Fig. 6); it will, however, be clear that the procedure is directly extended to the four-phase case. Referring to Fig. 6, (57) is written explicitly as

$$\dot{v}_{C_I} = \frac{1}{C}\left[-\frac{v_{C_I}}{R} + i_i\left(v_{C_I}\right)\right] - \frac{i_{L_I}}{C} - \frac{i_q(v_{C_Q})}{C} \tag{63}$$

$$\dot{i}_{L_I} = \frac{1}{L} v_{C_I} \tag{64}$$

$$\dot{v}_{C_Q} = \frac{1}{C}\left[-\frac{v_{C_Q}}{R} + i_i\left(v_{C_Q}\right)\right] - \frac{i_{L_Q}}{C} + \frac{i_q\left(v_{C_I}\right)}{C} \tag{65}$$

$$\dot{i}_{L_Q} = \frac{1}{L} v_{C_Q} \tag{66}$$

where $i_i(v_{C_I})$ $(i_i(v_{C_Q}))$ is the in-phase current injected by v_{C_I} (v_{C_Q}) into the I-tank (Q-tank), while $i_q(v_{C_I})(i_q(v_{C_Q}))$ is the quadrature current injected by v_{C_I} (v_{C_Q}) into the Q-tank (I-tank). The directions of $i_q(v_{C_I})$ and $i_q(v_{C_Q})$ in Fig. 6 correspond to the signs of the coupling between the two differential oscillators in Fig. 1.

We assume that i_i saturates at $\pm I_{B,\mathrm{sw}}$, and that i_q saturates at $\pm I_{B,\mathrm{cpl}} = \pm k I_{B,\mathrm{sw}}$. If the commutations between the positive and the negative current levels (and viceversa) are switch-like, and if the Q of the tank is high enough, it is well known that, with arbitrary initial phase, the approximate solution of the equation system above is

$$v_{C_I} = A\sin(\omega_1 t) \tag{67}$$

$$i_{L_I} = -\frac{A}{L\omega_1}\cos(\omega_1 t) \tag{68}$$

$$v_{C_Q} = -A\cos(\omega_1 t) \tag{69}$$

$$i_{L_Q} = -\frac{A}{L\omega_1}\sin(\omega_1 t) \tag{70}$$

where all current harmonics except the fundamental have been discarded. Moreover, the oscillation amplitude A is[4]

$$A = \frac{4}{\pi} R I_{B,\mathrm{sw}} \tag{71}$$

while the angular frequency of oscillation ω_1 is [11], [14]

$$\omega_1^2 - \omega_1 \frac{k}{RC} - \omega_0^2 = 0 \rightarrow \omega_1 \approx \omega_0 + \frac{k}{2RC} \tag{72}$$

where

$$\omega_0 = \frac{1}{\sqrt{LC}} \tag{73}$$

is the natural angular frequency of oscillation.[5]

From (58) and (63)–(66), DF is found without difficulty as shown in (74), at the bottom of the page, and equation system (59) is then written immediately as

$$\dot{y}_{C_I} = -y_{C_I}\left[-\frac{1}{RC} + \frac{1}{C}\frac{\partial i_i\left(v_{C_I}\right)}{\partial v_{C_I}}\right] - \frac{y_{L_I}}{L} - \frac{y_{C_Q}}{C}\frac{\partial i_q\left(v_{C_I}\right)}{\partial v_{C_I}} \tag{75}$$

$$\dot{y}_{L_I} = \frac{1}{C} y_{C_I} \tag{76}$$

[4]Equation (17) gives an amplitude double the one in (16). This is correct, since the in-phase current injected into the tanks in Fig. 6 switches between $I_{B,\mathrm{sw}}$ and $-I_{B,\mathrm{sw}}$, while the in-phase current injected into the tanks in Fig. 1 switches between $I_{B,\mathrm{sw}}$ and zero.

[5]In reality, a second solution set to (63)–(66) is possible, where $\omega_1 \approx \omega_0 - k/(2CR)$. Since the oscillator invariably chooses the condition (72), [14], we treat only such a state.

$$\mathrm{DF} = \begin{pmatrix} -\frac{1}{RC} + \frac{1}{C}\frac{\partial i_i(v_{C_I})}{\partial v_{C_I}} & -\frac{1}{C} & -\frac{1}{C}\frac{\partial i_q(v_{C_Q})}{\partial v_{C_Q}} & 0 \\ \frac{1}{L} & 0 & 0 & 0 \\ \frac{1}{C}\frac{\partial i_q(v_{C_I})}{\partial v_{C_I}} & 0 & -\frac{1}{RC} + \frac{1}{C}\frac{\partial i_i(v_{C_Q})}{\partial v_{C_Q}} & -\frac{1}{C} \\ 0 & 0 & \frac{1}{L} & 0 \end{pmatrix} \tag{74}$$

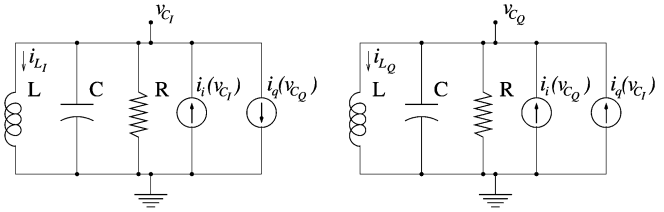

Fig. 6. Single-ended model for a quadrature oscillator.

$$\dot{y}_{C_Q} = \frac{y_{C_I}}{C}\frac{\partial i_q(v_{C_Q})}{\partial v_{C_Q}} - y_{C_Q}\left[-\frac{1}{RC} + \frac{1}{C}\frac{\partial i_i(v_{C_Q})}{\partial v_{C_Q}}\right] - \frac{y_{L_Q}}{L} \tag{77}$$

$$\dot{y}_{L_Q} = \frac{1}{C}y_{C_Q}. \tag{78}$$

The factors $\partial i_i(v_{C_I})/\partial v_{C_I}, \partial i_q(v_{C_I})/\partial v_{C_I}$, $\partial i_q(v_{C_Q})/\partial v_{C_Q}$, and $\partial i_i(v_{C_Q})/\partial v_{C_Q}$, are found exploiting the switch-like commutations of the currents. Considering e.g., $\partial i_i(v_{C_I})/\partial v_{C_I}$, we assume that $i_i(v_{C_I})$ switches from $-I_{B,\mathrm{sw}}$ to $I_{B,\mathrm{sw}}$ (and viceversa) over a very brief time Δt (brief compared of course to the oscillation period; see Fig. 7). Thus, over the commutation around $t = 0$, we can write

$$\frac{\partial i_i\,(v_{C_I})}{\partial v_{C_I}} = \frac{\partial i_i\,(v_{C_I})}{\partial t}\frac{\partial t}{\partial v_{C_I}} \approx \frac{2I_{B,\mathrm{sw}}}{\Delta t}\frac{1}{A\omega_1\cos(\omega_1 t)} \approx \frac{2I_{B,\mathrm{sw}}}{\Delta t}\frac{1}{A\omega_1} = \frac{1}{\Delta t}\frac{\pi}{2\omega_1 R} \tag{79}$$

where we have made use of (67) and (71). It is now straightforward to check that the same expression for $\partial i_i(v_{C_I})/\partial v_{C_I}$ is valid for the transition from $I_{B,\mathrm{sw}}$ to $-I_{B,\mathrm{sw}}$. In the limit of $\Delta t \to 0$, we can write the expression of $\partial i_i(v_{C_I})/\partial v_{C_I}$ over the whole oscillation period as

$$\frac{\partial i_i\,(v_{C_I})}{\partial v_{C_I}} = \frac{\pi}{2}\frac{1}{\omega_1 R}\left[\delta(t) + \delta\left(t - \frac{T}{2}\right)\right] \tag{80}$$

where $\delta(t)$ is Dirac's delta function. The other derivatives are found with the same procedure, and are

$$\frac{\partial i_q\,(v_{C_I})}{\partial v_{C_I}} = \frac{\pi}{2}\frac{k}{\omega_1 R}\left[\delta(t) + \delta\left(t - \frac{T}{2}\right)\right] \tag{81}$$

$$\frac{\partial i_i(v_{C_Q})}{\partial v_{C_Q}} = \frac{\pi}{2}\frac{k}{\omega_1 R}\left[\delta\left(t - \frac{T}{4}\right) + \delta\left(t - \frac{3T}{4}\right)\right] \tag{82}$$

$$\frac{\partial i_q(v_{C_Q})}{\partial v_{C_Q}} = \frac{\pi}{2}\frac{1}{\omega_1 R}\left[\delta\left(t - \frac{T}{4}\right) + \delta\left(t - \frac{3T}{4}\right)\right]. \tag{83}$$

We now make the informed guess that the solutions to (75) and (77), respectively, are

$$y_{C_I} \approx B\cos(\omega_1 t + \Psi) \tag{84}$$

$$y_{C_Q} \approx B\sin(\omega_1 t + \Psi) \tag{85}$$

which, through (76) and (78), yield immediately

$$y_{L_I} \approx \frac{B}{\omega_1 C}\sin(\omega_1 t + \Psi) \tag{86}$$

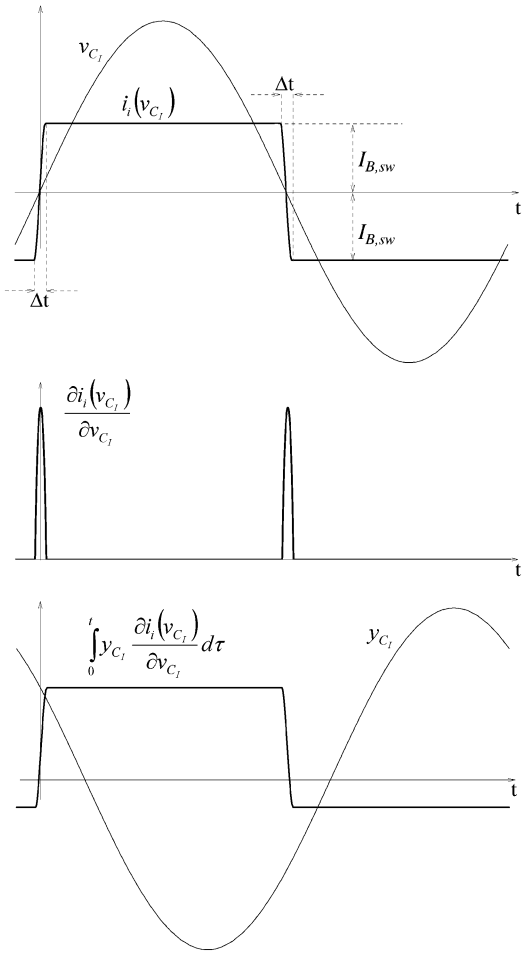

Fig. 7. Waveforms for the calculation of (88), where $\partial i_i(v_{C_I})/\partial v_{C_I}$ is well approximated by two Dirac's delta functions.

$$y_{L_Q} \approx -\frac{B}{\omega_1 C}\cos(\omega_1 t + \Psi). \tag{87}$$

Equation (75) (and (77) can now be solved for Ψ. Actually, due to the presence of the delta functions, it is easier to solve the integral of the two sides of (75). As an example, let us consider the integration of the factor $y_{C_I}\cdot\partial i_i(v_{C_I})/\partial v_{C_I}$ in (75)

$$\begin{aligned}\int_0^t y_{C_I}\frac{\partial i_i\,(v_{C_I})}{\partial v_{C_I}}d\tau &= \frac{\pi}{2}\frac{1}{\omega_1 R}\int_0^t B\cos(\omega_1\tau + \Psi)\left[\delta(\tau) + \delta\left(\tau - \frac{T}{2}\right)\right]d\tau \\ &= \overline{dc} + \frac{\pi}{2}\frac{B}{\omega_1 R} \\ &\quad\times\left(\cos(\Psi)u(t) + \cos(-\pi + \Psi)u\left(t - \frac{T}{2}\right)\right) \\ &= \overline{dc} + \frac{\pi}{2}\frac{B\cos(\Psi)}{\omega_1 R}\left(u(t) - u\left(t - \frac{T}{2}\right)\right)\end{aligned} \tag{88}$$

where $u(t)$ is the unit-step function, and $\overline{dc}$ a nonzero dc value in general. Fig. 7 shows the waveforms for all relevant functions appearing in (88). The term $u(t) - u(t - T/2)$ in (88) represents

a square wave with levels 1 and 0 and a 50% duty cycle, and can be expressed with its Fourier series as

$$u(t) - u\left(t - \frac{T}{2}\right) = \frac{1}{2} + \sum_{n\,\text{odd}} \frac{2}{n\pi} \sin(n\omega_1 t). \tag{89}$$

From (88) and (89), the time-varying expression[6] of (88) becomes

$$\int_0^t y_{C_I} \frac{\partial i_i\,(v_{C_I})}{\partial v_{C_I}} d\tau = \frac{B\cos(\Psi)}{\omega_1 R} \sum_{n\,\text{odd}} \frac{1}{n} \sin(n\omega_1 t). \tag{90}$$

Applying the same procedure to the factor $y_{C_Q} \cdot \partial i_q(v_{C_I})/\partial v_{C_I}$ in (75), the same (75) is easily integrated as

$$\begin{aligned} &B\cos(\omega_1 t + \Psi) \\ &\quad = \frac{B}{\omega_1 RC} \sin(\omega_1 t + \Psi) - \frac{B\cos(\Psi)}{\omega_1 RC} \sum_{n\,\text{odd}} \frac{1}{n} \sin(n\omega_1 t) \\ &\qquad + \frac{B}{\omega_1^2 LC} \cos(\omega_1 t + \Psi) \\ &\qquad - k\frac{B\cos(\Psi)}{\omega_1 RC} \sum_{n\,\text{odd}} \frac{1}{n} \sin(n\omega_1 t). \end{aligned} \tag{91}$$

Discarding again all harmonics except the fundamental, we obtain

$$\begin{aligned} &B\cos(\omega_1 t + \Psi) \\ &\quad = \frac{B}{\omega_1 RC} \sin(\omega_1 t + \Psi) - \frac{B}{\omega_1 RC} \cos(\Psi)\sin(\omega_1 t) \\ &\qquad + \frac{B}{\omega_1^2 LC} \cos(\omega_1 t + \Psi) \\ &\qquad - k\frac{B}{\omega_1 RC} \sin(\Psi)\sin(\omega_1 t) \end{aligned} \tag{92}$$

which, exploiting (72), can be simplified as

$$\begin{aligned} k\cos(\omega_1 t + \Psi) = \sin(\omega_1 t + \Psi) - \cos(\Psi)\sin(\omega_1 t) \\ -k\sin(\Psi)\sin(\omega_1 t) \end{aligned} \tag{93}$$

from which (4) easily follows, repeated here

$$\Psi = \arctan(k). \tag{94}$$

Equation (77) should be solved as well, since it might very well be that (94) is not compatible with (77). However, repeating the procedure just used for solving (75), it is simple to check that (94) is indeed a requirement for (77) as well.

There remains to find the factor B. Using (60), (67)–(70), and (84)–(87), we obtain

$$\begin{aligned} 1 = {} & AB\omega_1 \sin(\omega_1 t)\sin(\omega_1 t + \Psi) \\ & + AB\frac{\omega_0^2}{\omega_1} \cos(\omega_1 t)\cos(\omega_1 t + \Psi) \\ & + AB\omega_1 \cos(\omega_1 t)\cos(\omega_1 t + \Psi) \\ & + AB\frac{\omega_0^2}{\omega_1} \sin(\omega_1 t)\sin(\omega_1 t + \Psi) \end{aligned} \tag{95}$$

[6]The overall dc value in (88) is discarded, as we are here only interested in the fundamental component in each y_i.

from which

$$B \approx \frac{1}{2A\omega_1 \cos(\Psi)} \tag{96}$$

follows, given that $\omega_1 \approx \omega_0$. It is clear that the factor 2 at the denominator of (96) results from the number of phases generated in the oscillator. Thus, in presence of differential quadrature phases, this factor would be replaced with a factor 4. Calling this factor N in general, and substituting (84)–(85) and (96) in (62), we obtain finally (5)–(6), repeated below,

$$\Gamma_{I+}(\phi) = \frac{1}{N\cos(\Psi)} \cos(\phi + \Psi) \tag{97}$$

$$\Gamma_{Q+}(\phi) = \frac{1}{N\cos(\Psi)} \sin(\phi + \Psi) \tag{98}$$

which is the result we set out to demonstrate in this Appendix.

REFERENCES

[1] C. Samori, A. L. Lacaita, F. Villa, and F. Zappa, "Spectrum folding and phase noise in *LC* tuned oscillators," *IEEE Trans. Circuits Syst. II, Analog Digit. Signal Process.*, vol. 45, no. 7, pp. 781–790, Jul. 1998.

[2] J. J. Rael and A. Abidi, "Physical processes of phase noise in differential *LC* oscillators," in *Proc. CICC'00*, May 2000, pp. 569–572.

[3] P. Andreani, "Phase noise analysis of the *LC*-tank CMOS oscillator," in *Proc. IEEE Norchip'04*, Nov. 2004, pp. 147–150.

[4] P. Andreani, X. Wang, L. Vandi, and A. Fard, "A study of phase noise in colpitts and *LC*-tank CMOS oscillators," *IEEE J. Solid-State Circuits*, vol. 40, no. 5, pp. 1107–1118, May 2005.

[5] S. Levantino, C. Samori, A. Bonfanti, S. L. J. Gierkink, A. Lacaita, and V. Boccuzzi, "Frequency dependence on bias current in 5 GHz CMOS VCOs: Impact on tuning range and flicker noise upconversion," *IEEE J. Solid-State Circuits*, vol. 37, no. 8, pp. 1003–1011, Aug. 2002.

[6] E. Hegazi and A. A. Abidi, "Varactor characteristics, oscillator tuning range, and AM-FM conversion," *IEEE J. Solid-State Circuits*, vol. 38, no. 6, pp. 1033–1039, Jun. 2003.

[7] X. Wang and P. Andreani, "A phase noise analysis of the CMOS colpitts oscillator," in *Proc. IEEE Norchip'04*, Nov. 2004, pp. 151–154.

[8] A. Rofougaran, J. Rael, M. Rofougaran, and A. Abidi, "A 900-MHz CMOS *LC*-oscillator with quadrature outputs," in *Proc. ISSCC'96*, Feb. 1996, pp. 392–393.

[9] P. Vancorenland and M. Steyaert, "A 1.57 GHz fully integrated very low phase noise quadrature VCO," *IEEE J. Solid-State Circuits*, vol. 37, no. 5, pp. 653–656, May 2002.

[10] J. van der Tang, P. van de Ven, D. Kasperkovitz, and A. van Roermund, "Analysis and design of an optimally coupled 5-GHz quadrature *LC* oscillator," *IEEE J. Solid-State Circuits*, vol. 37, no. 5, pp. 657–661, May 2002.

[11] P. Andreani, A. Bonfanti, L. Romanò, and C. Samori, "Analysis and design of a 1.8-GHz CMOS *LC* quadrature VCO," *IEEE J. Solid-State Circuits*, vol. 37, no. 12, pp. 1737–1747, Dec. 2002.

[12] S. L. J. Gierkink, S. Levantino, R. C. Frye, and V. Boccuzzi, "A low-phase-noise 5-GHz CMOS quadrature VCO using superharmonic coupling," *IEEE J. Solid-State Circuits*, vol. 38, no. 7, pp. 1148–1154, Jul. 2003.

[13] P. Andreani and X. Wang, "On the phase-noise and phase-error performances of multiphase LC CMOS VCOs," *IEEE J. Solid-State Circuits*, vol. 39, no. 11, pp. 1883–1893, Nov. 2004.

[14] L. Romanò, S. Levantino, A. Bonfanti, C. Samori, and A. L. Lacaita, "Phase noise and accuracy in quadrature oscillators," in *Proc. IEEE ISCAS'04*, May 2004, vol. 1, pp. 161–164.

[15] A. Hajimiri and T. H. Lee, "A general theory of phase noise in electrical oscillators," *IEEE J. Solid-State Circuits*, vol. 33, no. 2, pp. 179–194, Feb. 1998.

[16] A. Mazzanti, F. Svelto, and P. Andreani, "On the amplitude and phase errors of quadrature *LC*-tank CMOS oscillators," *IEEE J. Solid-State Circuits*, vol. 41, no. 6, pp. 1305–1313, Jun. 2006.

[17] A. Hajimiri and T. H. Lee, "Corrections to "A general theory of phase noise in electrical oscillators"," *IEEE J. Solid-State Circuits*, vol. 33, no. 6, p. 928, Jun. 1998.
[18] F. X. Kärtner, "Determination of the correlation spectrum of oscillators with low phase noise," *IEEE Trans. Microw. Theory Tech.*, vol. 37, no. 1, pp. 90–101, Jan. 1989.
[19] ——, "Analysis of white and $f^{-\alpha}$ noise in oscillators," *Int. J. Circuit Theory Appl.*, vol. 18, pp. 485–519, 1990.

Pietro Andreani received the M.S.E.E. degree from the University of Pisa, Pisa, Italy, and the Ph.D. degree from Lund University, Lund, Sweden, in 1988 and 1999, respectively.

He was with the Department of Applied Electronics (now Department of Electroscience), Lund University, between 1990 and 1993, and again between 1995 and 2001, as an Associate Professor, when he was responsible for the Analog IC courses. Since 2001, he has been a Professor at the Center for Physical Electronics, ØrstedċDTU, Technical University of Denmark, Kgs. Lyngby, Denmark, with analog/RF IC design as his main research field.